INFLUENCE OF TOOL-PART FRICTIONAL INTERACTION ON THE CURE-INDUCED DEFORMATIONS IN THERMOSET-BASED COMPOSITE PARTS

Antoine Parmentier and David Dumas

Cenaero ASBL, Centre de recherche en aéronautique
Bâtiment Eole, Rue des Frères Wright 29, B-6041 Gosselies, Belgium
E-mail: antoine.parmentier@cenaero.be, web page: http://www.cenaero.be

Keywords: Composite, Simulation, Cure, Distortion, Warpage

ABSTRACT

The friction between the tool and the composite part during curing is known to have a significant influence on the final shape of the part which is a direct consequence of mismatch in the coefficients of thermal expansion between the mould and the composite part. With the development of closed mould processes such as Resin Transfer Moulding (RTM), the complexity of the moulds have increased resulting steep rise in manufacturing costs. Aluminium moulds are therefore more commonly used to reduce their cost but induce significant cure-induced deformations. The present numerical study aims at determining the influential parameters when predicting cure-induced warpage of flat plates. The model has been validated through simulations of flat plates with different fiber orientations, thicknesses and manufactured on moulds of different materials. The sensitivity analysis results have shown the importance of accurately determining the parameters of the Coulomb's law, the friction coefficient and the shear stress limit, to evaluate the warpage magnitude by simulations.

1 INTRODUCTION

The polymerisation reaction or curing, which transforms thermoset resins from liquid to solid state, induces internal stresses within the part being produced. During this change of state, the part experiences deformations due to thermal expansion and chemical shrinkage of the resin. These deformations are constrained from developing freely due to the interaction of the part with the mould and result in the build up of internal stresses. Upon demoulding, stresses on the newly free surface are released, resulting in the appearance of distortions. One of the main challenges with the development of curing models to accurately predict deformations and residual stresses is to identify the critical process physics which cannot be excluded from the modelling process. Previous research has shown that the friction between the tool and the composite part during curing is known to have a significant influence on the final shape of the part [1, 2]. This is a direct consequence of mismatch in the coefficients of thermal expansion (CTE) between the mould and the composite part. In order to reduce the influence of the tool-part interaction on the distortions, composite parts with tight dimensional tolerances are manufactured on Invar tooling which is notable for its uniquely low thermal expansion. However, the use of Invar is reserved for specific parts due to its high cost and the difficulty to machine it. With the development of closed mould processes such as Resin Transfer Moulding (RTM), the complexity of the moulds have increased resulting in steep rise in manufacturing costs. Therefore, aluminium moulds are more commonly used to reduce their cost. However, the difference of CTE between aluminium and thermoset resins is significantly high which results in larger cure-induced deformations. This brings about an interest in being able to predict these distortions in order to compensate the mould geometry and respect tight dimensional tolerances

The present study aims at determining the friction parameters which need to be taken into account in curing simulations when modelling the frictional tool-part interaction. A sensitivity analysis has been performed in order to identify the influential parameters and to help determine the accuracy with which those parameters have to be measured experimentally. Different experimental methodologies

have been developed in [3-5] in order to measure friction parameters during curing with different levels of complexity. The sensitivity analysis will help identify which method is most suitable.

The specific cure-induced deformation behaviour of interest is the warpage measured as the deflection between the center point of the plates and a point located in the middle of an edge.

2 MATERIALS AND METHOD

The materials of interest are the unidirectional (UD) and plain-weave fabric carbon/epoxy prepregs AS4/8552 produced by Hexcel. The reference stacking sequence is made of 8 plies of prepregs and the parts modelled are considered to be manufactured on an aluminium mould with a coefficient of thermal expansion (CTE) of 24E-06 [1/°C]. The cure cycle applied in the simulation is the Manufacturer's Recommended Cure Cycle (MRCC) which consists in a heating ramp of 2°C/min from the room temperature to 120°C. This temperature is held for 60min before a second heating ramp to 180°C at a rate of 2°C/min. The part then cures at this temperature for 120min before cooling to room temperature at a rate of 2°C/min. A pressure of 7 bars is applied through the whole duration of the cycle.

The numerical prediction methodology used consists of performing coupled chemical-thermal-mechanical Finite Elements (FE) calculations using ABAQUS with the help of user material subroutines. It was assumed that the temperature gradient across the thickness of the part was negligible due to the low thickness of the part. As a result, a transient thermal analysis was not performed and the temperature was considered to be uniform throughout the part. The model follows the approach proposed by Svanberg and Holmberg [6] who consider a simplified linear viscoelastic behaviour of the material where time-temperature-degree of cure superposition is invoked. Two of the main assumptions made are: (i) the thermal expansion is assumed to be linear within each material state, and (ii) the material properties are kept constant for each state, viscous, rubbery or glassy, of the resin. The material properties used for numerical simulations of parts made of UD prepregs are those used in [7, 8] and presented in Table 1. Material's CTE at rubbery and glassy state (except the transverse coefficient) have been determined using micromechanics equations with fibres and matrix properties. The evolution of the chemical shrinkage with the degree of cure X has been determined in [9] :

$$\varepsilon_{cure}(X) = 2.16X^3 - 1.62X^2 - 2.70X + 0.93 \quad (1)$$

The transition from the viscous to the rubbery state is defined at a degree of cure of 0.31 [10] . The transition between the rubbery and the glassy state happens when the resin temperature reaches its glass transition temperature Tg which is assumed to depend only on the degree of cure X. The model used to predict the glass transition temperature Tg as a function of the degree of cure X is the one used in [9] as illustrated in the following equations:

$$Tg(X) = 164.6X^2 + 51.0X + 2.67 \quad (2)$$

where the degree of cure X is computed from the cure kinetic law:

$$\frac{dX}{dt} = \frac{70000e^{\left(-65000/RT\right)}X^{0.5}(1-X)^{1.5}}{1+e^{30\left(X+1.5148-5.171*10^{-3}T\right)}} \quad (3)$$

where X, R and T are the degree of cure, the gas constant and the cure temperature in Celsius degrees, respectively.

The prepreg is initially at viscous state and the resin is not able to sustain any stress. Since the autoclave pressure keeps the material against the mould, the fibres are stretched due to the CTE mismatch between the fibres and the aluminium mould as illustrated on Figure 1. A shear stress therefore develops at the interface which creates a stress gradient in the thickness of the part. The

associated deformation is locked in the part while curing and lead upon demoulding to the warpage. This viscous state is therefore modelled in the present work, following the approach presented in [7, 11]. The composite is considered to be unable to sustain any stress related to thermal expansion or chemical shrinkage before gelation.

Properties		Viscous	Rubbery	Glassy
E_1	[MPa]	132200	132200	135000
E_2=E_3	[MPa]	165	165	9500
G_{12}=G_{13}	[MPa]	44.3/5	44.3	5490
G_{23}	[MPa]	41.6/5	41.6	3272
ν_{12}=ν_{13}	–	0	0.346	0.3
ν_{23}	–	0	0.982	0.45
α_1	[1/°C]	0	-8.80E-07	-1.55E-07
α_2=α_3	[1/°C]	0	1E-04	32.6E-06

Table 1: Material properties used in the numerical model for the UD prepreg of 8552/AS4 [7, 8]. Subscripts 1 indicates the fibres direction. α stands for the coefficients of thermal expansion.

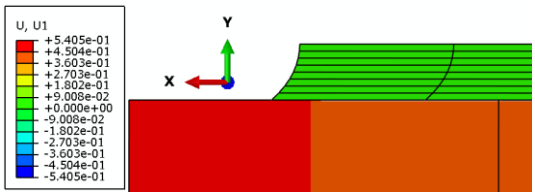

Figure 1: Horizontal displacement illustrating the shear deformation induced by the frictional tool-part interaction at the viscous state (Displacements shown in milimeters).

The numerical model ability to represent the influence of the tool-part frictional interaction has been evaluated on modeling the deformations of flat plates manufactured by the autoclave process. The flat plates dimensions are 300mm*300mm with 8 plies stacked at different orientations. The process is modelled by applying boundary conditions intended to be close to those encountered experimentally in the autoclave: a pressure is applied on the free surface of the part to account for the effect of the autoclave, and the tool is modelled as a deformable body. The autoclave pressure constrains the part against the mould and the mould prevents the part from warping during cure. The frictional interaction between the aluminium mould and the part has been modelled using the Coulomb friction law with a constant friction coefficient: the shear stress at the interface is proportional to the normal pressure. The coefficient of proportionality is the static friction coefficient μ. Due to the relative displacement between the part and the tool, the shear stress at the interface arises. A shear stress limit τ_{max} has been defined which is the maximum stress the interface can carry before a sliding motion develops between the tool and the part. The tool-part friction coefficient and the maximum shear stress have been taken from [12] .

The influence of the stacking sequence on the warpage pattern is studied and a sensitivity analysis evaluates the influence of the part thickness, friction parameters and mould material on the warpage magnitude.

3 RESULTS AND DISCUSSION

Simulations of flat plates of differents materials helped to qualitatively validate the numerical tool by evaluating the influence of the fiber arrangment and stacking sequence on the pattern of warpage. Three simulations of parts with the following stacking sequences and denominations have been analysed:

- 8 plies of UD prepreg oriented in the 0° direction or x-direction: $[0°]_8$
- 8 plies of UD prepreg with a cross-ply stacking sequence (XP): $[0°/90°]_{2s}$

– 8 plies of prepreg fabric: $[0°\text{-}90°]_8$

The patterns predicted by the simulations are presented in Figure 2. The UD stacking sequence (Figure 2a) shows a single curvature along the fibers directions while iso-contours are observed in the in-plane direction transverse to the fibers. For the fabric stacking sequence (Figure 2c), the warpage is similar to all in-plane directions and characterized by circular iso-contours. The XP stacking sequence (Figure 2b) lies between the two previous cases: the warpage in the x-direction is slightly more important which shows the influence of the fibre orientation of the ply in direct contact with the mould on the deformation. These observations are in line with those reported in [13] .

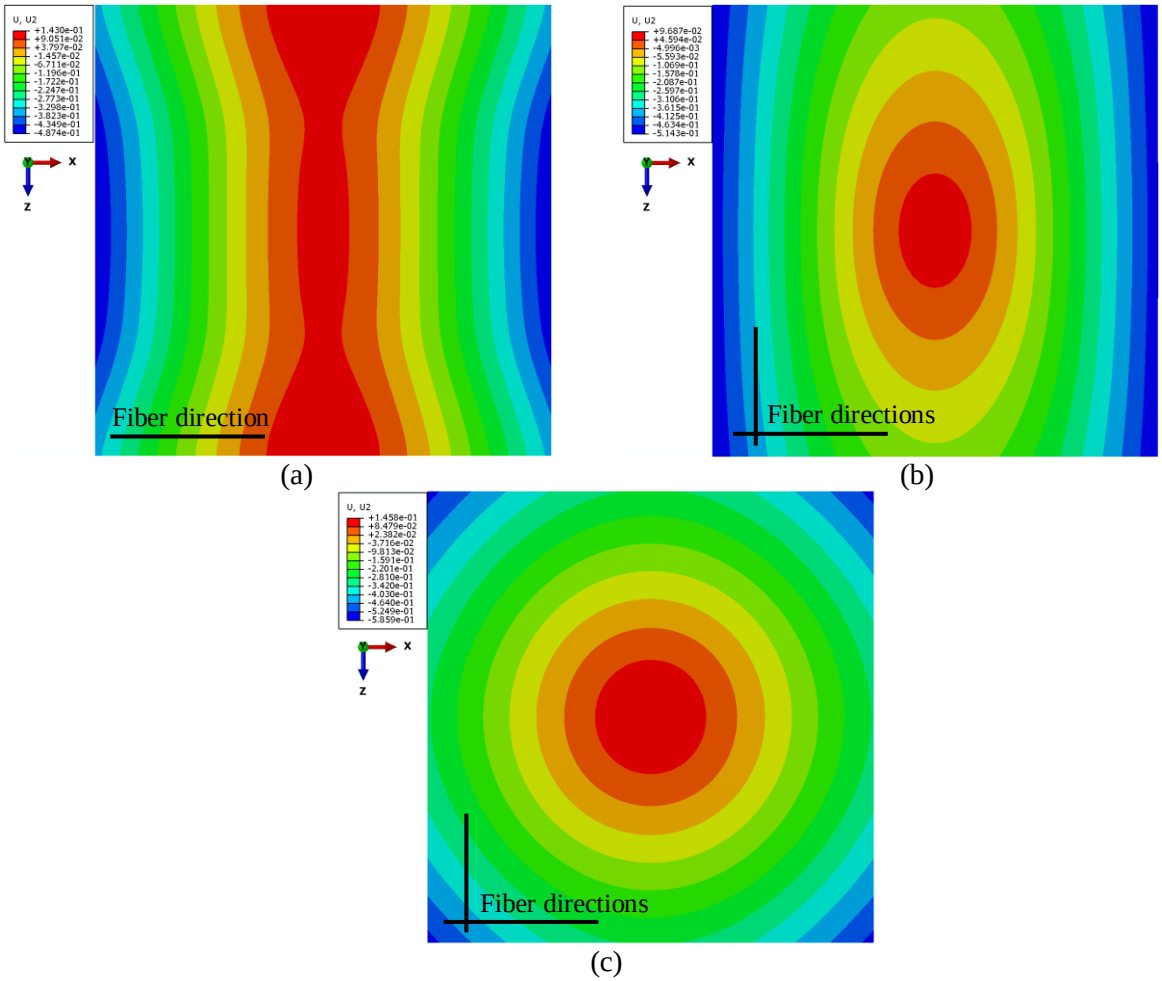

Figure 2: Influence of the fibres arrangment and materials to the pattern of the warpage: (a) unidirectional $[0°]_8$, (b) cross-ply $[0°/90°]_{2s}$ and (c) fabric $[0°\text{-}90°]_8$. The displacement transverse to the plate is presented.

A sensitivity analysis has been performed in order to identify the influential parameters when predicting cure-induced distortions. The warpage magnitudes presented in the following sub-sections are normalized by a “reference case” which is the warpage presented on the red bars of each graph. This helps better visualize the influence of the parameter modification on the warpage magnitude.

3.1 Influence of the part thickness

The warpage predictions for plain weave composite of different thicknesses are given in Figure 3. For relatively thin composites of 4 to 12 plies, the warpage magnitude increases with the part thickness. This is related to the increase of the stress gradient in the thickness direction with an increase of the number of plies. Compared to the reference case (8 plies), reducing the number of plies

by two shows a drop in the warpage magnitude of roughly 55%. Increasing the ply number by 50% tends to increase the warpage by 22%. However, for thicker composite of 24 plies, the increased bending stiffness of the part tends to reduce the warpage. When the bending stiffness is greater than the increase of locked-in stress gradient in the composite thickness, the warpage begins to drop with the number of plies.

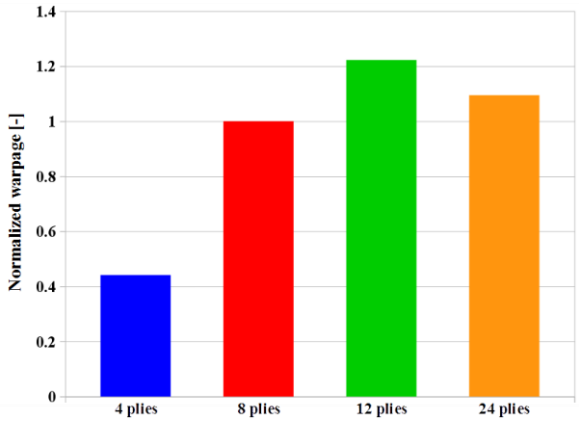

Figure 3: Influence of the part thickness on the warpage magnitude for carbon fabric reinforced polymers.

3.2 Influence of the friction parameters

In order to model different interface conditions and to study the influence of friction parameters on the warpage magnitude, the static friction coefficient μ and the limiting shear stress τ_{max} have been varied. This would help determine the accuracy with which those parameters have to be measured experimentally to enrich quantitatively the numerical model at a later stage.

The static friction coefficient between two solid surfaces is defined as the ratio between the tangential force required to produce sliding and the normal force transmitted at the interface. The normal force develops due to the autoclave pressure applied on the free surface of the part. The influence of the static friction coefficient on the warpage magnitude is presented in Figure 4a where the limiting shear stress τ_{max} was set to 0.2 MPa. Decreasing the friction coefficient results in a reduction of the transmitted tangential force required to induce the tool-part slipping motion which therefore develops earlier in the cure. The residual stress locked in the part during cure is then lower too, resulting in less warpage, as observed when reducing μ from 0.5 (red) to 0.2 (blue) in Figure 4a. However, no difference is observed while varying the coefficient from 0.5 to 0.8. This can be explained using the Coulomb's friction law as shown in Figure 4b for different friction coefficient values: the shear stress at the tool-part interface increases linearly until it reaches the minimum values between the shear stress predicted by the Coulomb's law μP and the limiting shear stress τ_{max} (0.2 [MPa] in the present case) :

$$\tau = \min(\mu P, \tau_{max}) \tag{3}$$

where P, the normal stress transmitted at the interface (assumed to be the autoclave pressure of 0.7 [MPa]) represented by the solid black line on Figure 4b. For a friction coefficients of 0.2, the sliding motion occurs at a shear stress of 0.14 [MPa] (Coulomb's law) which is the intersection of the solid black and blue lines on Figure 4b. However, for a coefficient of friction of 0.5, the tool-part sliding starts as the shear stress reaches 0.2 [MPa] which is limiting the shear stress τ_{max} for the Coulomb's law. The sliding motion occurs later when switching the coefficient of friction from 0.2 to 0.5 and results in a significant increase in the warpage deformation as observed in Figure 4a. However, the difference in the initiation of the sliding motion between the coefficient of 0.5 and 0.8 vanishes as both have the tool-part sliding motion occuring at the limiting shear stress of 0.2 [MPa]: the solid black line does not cross the slopes of neither the red nor the green lines following the Coulomb's law. These

observations agree with the warpage predictions of Figure 4a.

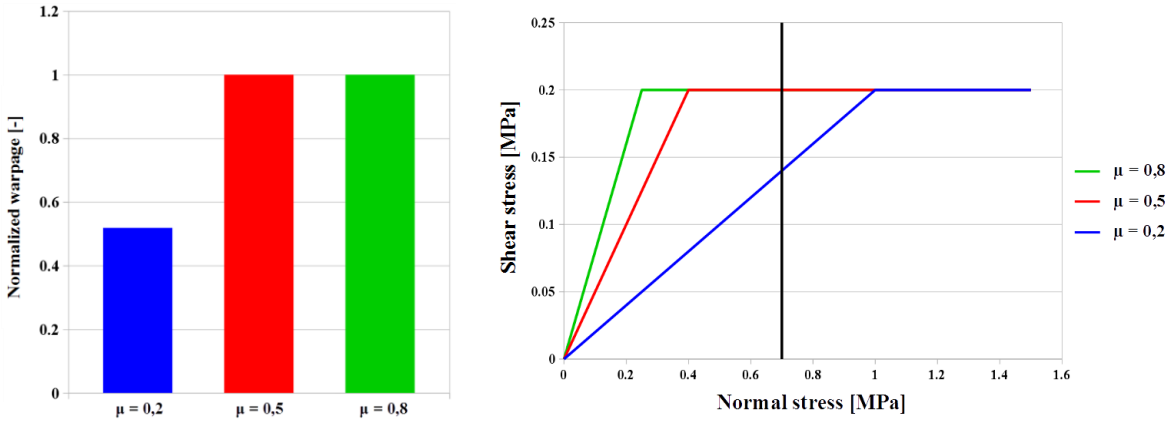

(a) (b)

Figure 4: (a) Influence of the static friction coefficient on the warpage magnitude (b) Coulomb's friction law for different static friction coefficients. The limiting shear stress is fixed at 0.2 [MPa].

The influence of the limiting shear stress τ_{max} on the warpage magnitude is presented in Figure 5a. This parameter defines the maximum shear stress the interface can carry before a sliding motion develops between the tool and the part. The predictions show that an increase in the limiting shear stress (at constant friction coefficient) tends to increase the warpage magnitude: the part remains in a sticking contact longer and accumulate more shear stress which results in a higher warpage upon demoulding. However, increasing the shear stress limit from 0.4 to 0.5 does not influence the warpage magnitude. This can be explained with the Coulomb's friction law in Figure 5b for several values of τ_{max}: both green and orange lines shows the stick-slip friction transition occuring at the same shear stress given by the Coulomb's law μP=0.35 [MPa] which gives the same warpage magnitude. The red and blue curves justify the simulation results: the sliding motion occurs much earlier fixing the τ_{max} at 0.05 than 0.2 which results in a significantly lower warpage magnitude.

The relative influence of the friction parameters μ and τ_{max} on the predictions of the warpage magnitude can be anticipated plotting the Coulomb's friction.

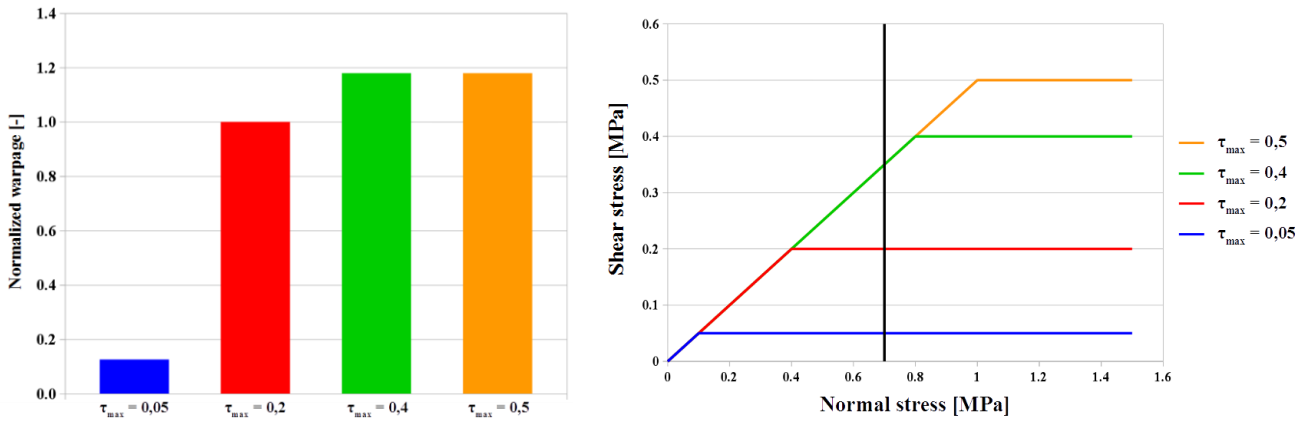

(a) (b)

Figure 5: (a) Influence of the shear stress limit on the warpage magnitude (b) Coulomb's friction law for different limiting shear stress [MPa]. The static friction coefficient is kept at 0.5.

3.3 Influence of the mould material

The warpage of parts is a direct consequence of mismatch in the coefficients of thermal expansion (CTE) between the mould and the composite part. The final shape of parts is therefore highly dependent of the mould material. The influence of the mould material on the warpage magnitude predictions is presented on Figure 6. The simulation of a mould made of Invar does not bring any warpage deformation while simulating a part made of plain weave fabric plies. This was expected as the CTE of Invar is close to the CTE of carbon prepreg in the fibre directions. However, for steel and aluminium materials whose CTE is significantly higher, a warpage of the plate is predicted. The expansion of the mould associated to a sticking contact at the beginning of the cure cycle put the fibers in tension. A shear stress develops at the interface and induces a stress gradient in the thickness direction which results upon demoulding in a warpage deformation. The warpage tends to slightly increase with an increase in the mould CTE from steel to aluminium eventhough the difference is not significant. Twigg et al. showed in [1] that the difference of the mould material on the warpage increase with the length of the part and becomes visible from 5m long parts, much longer than the plate modelled in the present study.

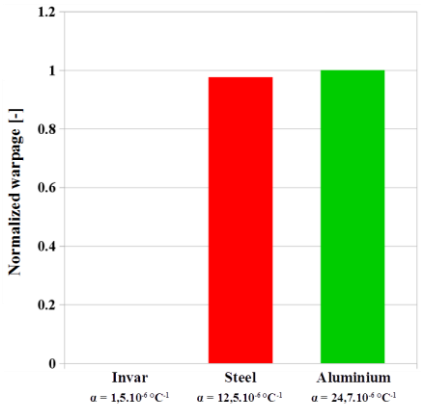

Figure 6: Influence of the mould material on the warpage magnitude

4 CONCLUSIONS

The numerical model reliability has been assessed modelling parts of different thicknesses and stacking sequences which are known to influence the cure-induced deformations. The results have shown variations in the warpage magnitude depending the part thickness and different warpage patterns following the stacking sequence. The predictions of the warpage patterns are in agreement with the observations reported in [7] . The model is also sensitive to the thermal expansion of the mould which is the root cause of the warpage deformation. The parts studied are not long enough to exhibit a significant difference between the warpage on parts produced with a steel or an aluminium mould.

The sensitivity analysis performed has highlighted the importance of the friction parameters, static friction coefficient and shear stress limit, in order to predict the warpage magnitude of parts accurately. Those parameters will be characterized carefully in a later stage and the predictions will be compared to experimental measurements in order to evaluate the accuracy of the numerical model. The comparison will help to assess the assumption of implementing constant friction parameters throughout the cure cycle.

ACKNOWLEDGEMENTS

The authors would like to thank the Walloon Region in Belgium and Skywin (Aerospace Cluster of Wallonia) for their financial support through the project TECCOMA. The authors also thank Yoan Bouyer from Ecole Centrale de Nantes (France) and Juan Vicente Fernandez Alba from Ecole Centrale de Lille (France) for their contribution to the present work.

REFERENCES

[1] G. Fernlund, G. Twigg and A. Poursartip, Tool-part interaction in composite processing Part 1: experimental investigation and analytical model, *Composites Part A: Applied Science and Manufacturing*, **35**, 2004, pp. 121-133 (doi: 10.1016/S1359-835X(03)00131-3).

[2] T. Garstka, Separation of process induced distortions in curved composite laminates, Ph.D. Thesis, University of Bristol, 2005.

[3] G. Twigg, A. Poursartip and G. Fernlund, An experimental method for quantifying tool-part shear interaction during composites processing, *Composites Science and Technology*, **63**, 2003, pp. 1985-2002 (doi: 10.1016/S0266-3538(03)00172-6).

[4] V. Kaushik and J. Raghavan, Experimental study of tool-part interaction during autoclave processing of thermoset polymer composite structures, *Composites Part A: Applied Science and Manufacturing*, **41**, 2010, pp. 1210-1218 (doi: 10.1016/j.compositesa.2010.05.003).

[5] L. Khoun, R. de Oliveira, V. Michaud and P. Hubert, Investigation of process-induced strains development by fibre Bragg grating sensors in resin transfer moulded composites, *Composites Part A: Applied Science and Manufacturing*, **42**, 2011, pp. 274-282 (doi: 10.1016/j.compositesa.2010.11.013).

[6] J.M. Svanberg and J.A. Holmberg, Predictions of shape distortions Part I. FE-implementation of a path dependent constitutive model, *Composites Part A: Applied Science and Manufacturing*, **35**, 2004, pp. 711-772 (doi: 10.1016/j.compositesa.2004.02.005).

[7] K. Cinar and N. Ersoy, 3D finite element model for predicting manufacturing distortions of composite parts, *Journal of Composite Materials*, **50**, 2016, pp. 3791-3807 (doi: 10.1177/0021998315625789).

[8] N. Ersoy et al., Development of the properties of a carbon fibre reinforced thermosetting composite through cure, *Composites Part A: Applied Science and Manufacturing*, 41, 2010, pp. 401-409 (doi: 10.1016/j.compositesa.2009.11.007).

[9] N. Ersoy et al., Development of spring-in angle during cure of a thermosetting composite, *Composites Part A: Applied Science and Manufacturing*, **36**, 2005, pp. 1700-1706 (doi: 10.1016/j.compositesa.2005.02.013).

[10] T. Garstka et al., In situ measurements of the through-the-thickness strains during processing of AS4/8552 composite, *Composites Part A: Applied Science and Manufacturing*, 38, 2007, pp. 2517-2526 (doi: 10.1016/j.compositesa.2007.07.018).

[11] K. Cinar and al., Modelling manufacturing deformations in corner sections made of composite materials, Journal of Composite Materials, 48, 2014, pp. 799-813 (doi: 10.1177/0021998313477896).

[12] O. Ozgu et al., Numerical investigation of tool-part interactions in composites manufacturing, *Proceedings of the 16th International Conference on Composite Materials ICCM16, Kyoto, Japan, July 3-8, 2007*.

[13] O. Yuksel et al., Experimental and numerical study of the tool-part interaction in flat and double curvature parts, *Proceeding of the 17th European Conference on Composite Materials ECCM17, Munich, Germany, June 26-30, 2016.*